Area-Selective Formation of Macropore Array by Anisotropic Electrochemical Etching on an n-Si(100) Surface in Aqueous HF Solution

Takayuki Homma,*,† Hirotaka Sato,† Kentaro Mori,† Tetsuya Osaka,† and Shuichi Shoji‡

Department of Applied Chemistry and Department of Electrical Engineering and Bioscience, Waseda University, Okubo, Shinjuku, Tokyo 169-8555, Japan

Received: September 15, 2004; In Final Form: November 27, 2004

A photoassisted anodization process to fabricate arrays of uniform and straight macropores at selected areas of a Si wafer surface was developed. The front- and backside surfaces of n-type Si(100) wafers were coated with a thin Si_3N_4 layer, and the frontside layer was micro-patterned using photolithography and reactive ion etching to form an array of microscopic openings at selected areas. The inverted pyramid-shape micropits were formed at these openings by anisotropic etching using aqueous KOH solution; these pits act as the initiation sites for the anodization to form macropores. The electrochemical etching was carried out in aqueous HF solution under illumination from the backside of the wafer, on which Au/Cr electric contact was formed following removal of the Si_3N_4 layer. To improve the uniformity of the formation condition of the macropores at the selected area, holes were area-selectively generated by controlling the illumination condition during the anodization. For this, micropatterns were formed on the Au/Cr layer at the backside surface, which were aligned to those at the frontside surface. The parameters, such as HF concentration, current density, and wafer thickness, i.e., hole diffusion length, were optimized, and the arrays of uniform and high-aspect-ratio macropores were formed at the selected area of the domain at the silicon surface.

1. Introduction

The fabrication process of well-ordered or arrayed porous microstructure is significant to develop advanced devices, such as through hole interconnects and channels in three-dimensional electronic and fluidic devices, etc.[1−3] A dry etching process, such as reactive ion etching (RIE), has been mainly used for fabrication of these structures.[1−3] Recently, deep reactive ion etching (DRIE) was developed, which could form high-aspect-ratio structures by repeating an etching step and a protective step of fluorocarbon layer formation onto the etched pattern walls to prevent the side etching.[4−6] However, the DRIE is a high-cost process and has a limitation to achieve the higher aspect ratio up to 30−40. Furthermore, the walls formed by DRIE are not flat as a result of the stepwise process described above.

On the other hand, the Si anodization process, which is electrochemical dissolution of Si in aqueous HF solution, has been developed to achieve formation of high-aspect-ratio pores. Initially, it was found that the porous Si layer, consisting of nanometer-size branched pores, was formed during the anodization for the electropolishing process.[7,8] Since the porous Si layer is well-known to possess photo- and electroluminescence properties and can be oxidized 80−120 times faster than a conventional Si(100) layer, the porous Si has been extensively studied for the applications of luminescence devices and SOI (Silicon On Insulator) structures.[9−12] In addition to these properties, the pores are known to grow vertically to Si(100) facets.[13] By utilizing the anisotropic etching property of the Si anodization, a straight macropore array with a diameter of several micrometers and high aspect ratio (>100) could be formed using an n-type Si(100) wafer.[14−16] To form a straight macropore array, it is important to keep enhancing the dissolution reaction at the tip (bottom edge) part of the pores, which can be achieved by focusing the hole, which acts as one of the dissolution agents, to the tip part. However, such a "focusing" is difficult for p-type Si wafers because their major carriers are holes and are supplied not only to tip parts but also to the sidewall parts of the pores. On the other hand, a hole is a minority carrier in n-type Si wafers, so that it is possible to adjust the generation and diffusion condition of holes by illuminating and applying anodic bias.[17] By anodization assisted with backside illumination, holes are generated at the backside of the wafer and diffused toward the frontside by applying anodic bias, and by forming patterned micropits at the surface of the frontside prior to the Si anodization, which act as the initiation sites for the Si dissolution, the holes are focused to their tip part to achieve formation of the straight macropores at each micropit. By using this process, formation of a uniform array of the macropore to the entire surface of the substrate has been achieved.[14] On the other hand, for the fabrication of various microdevices and systems, arrays of the pores are required to be formed uniformly at "microscopically selected" areas according to their designs. However, such an area-selective formation has been difficult because holes diffuse to the reaction sites ununiformly due to its random walk diffusion and its accumulation around the edge of the selected area, resulting in nonuniform formation of the pores.[18−20] In this study, we attempt to fabricate a high-aspect-ratio macropore array at selected areas by modifying the Si anodization conditions, such as the hole generation region, supply rate, and diffusion length.

2. Experimental Section

Figure 1 shows the process steps for formation of the macropore array by Si anodization applied to this study. We

* Author to whom correspondence should be addressed. E-mail: homma@mse.waseda.ac.jp.

† Department of Applied Chemistry.

‡ Department of Electrical Engineering and Bioscience.

10.1021/jp045822n CCC: $30.25
Published on Web 03/04/2005

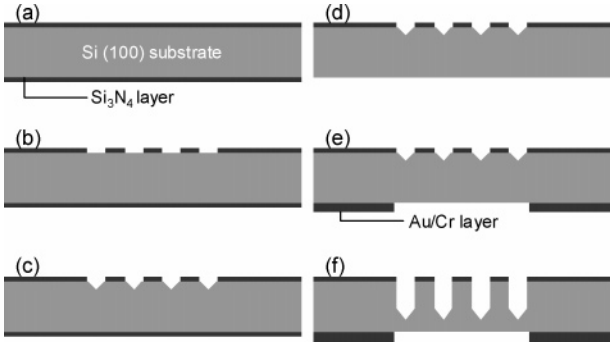

Figure 1. Process steps for the macropore array; (a) Si_3N_4 coating by LPCVD, (b) front surface patterning of Si_3N_4 by RIE, (c) anisotropic alkaline etching on the front surface, (d) back surface removal of Si_3N_4 by RIE, (e) Au/Cr evaporation and patterning onto the back surface, (f) Si anodization.

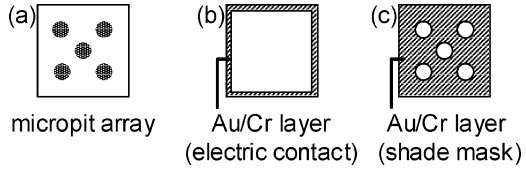

Figure 2. Schematic designs of the substrate for the Si anodization, (a) front surface view, (b) rim-type Au/Cr pattern, (c) shade mask Au/Cr pattern.

TABLE 1: Electrolyte Composition and Operating Conditions of Si Anodization

chemicals	
HF	0.1−10 wt %
C_2H_5OH	8.15 wt %
current density	0.24-24 mA/cm^2
bath temperature	Room temperature
counter electrode	Pt
reference electrode	Ag/AgCl

used 200−625-μm thick n-type Si(100) wafers with 5 Ω cm specific resistance, whose front- and backside surfaces were coated with a 140 nm thick Si_3N_4 layer by low-pressure chemical vapor deposition (LPCVD), which act as the resistant layer for wet etching. The wafer was cut into square pieces (20 mm × 20 mm), and the Si_3N_4 layer was patterned using photolithography and RIE. Using the micropatterned Si_3N_4 layer as a protective mask, inverted pyramid-shape micropits were formed by anisotropic etching using a 20 wt % KOH solution at 90 °C. The micropits serve as the initiation sites for the anodization to form macropores. The patterned side of the pyramid is 10-μm-square, and approximately 2000 pits were arranged at an interval of 10 μm in a 1000-μm-diameter area on the substrate, where the five domains were formed to examine the area-selective formation, as is shown in Figure 2a. After the anisotropic etching to form the initiation sites, the Si_3N_4 layer on the backside was removed by RIE, and two types of Au/Cr patterns were formed as a conductive layer for the anodization process, as is shown in Figure 2b and 2c. The roles of Au/Cr patterns will be explained later. For the anodization process, a specimen with the initiation sites at the front surface and the Au/Cr pattern at the back surface was mounted on the bottom of the electrochemical cell using a copper holder, which was electrically connected to a potentiostat/galvanostat (Hokuto-Denko, HA-501). Table 1 shows electrolyte composition and operating conditions of the Si anodization. Current density was defined by considering the amount of surface area of an inverted pyramid-shape micropit as the normalized area. During the anodization, the back surface of the specimen was illuminated

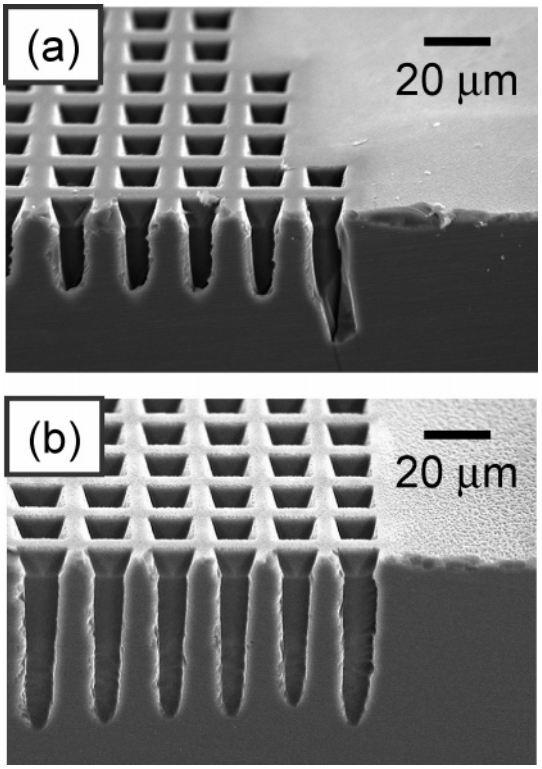

Figure 3. Cross-sectional SEM images showing the formation condition of the pores; (a) without the shade mask; (b) with micropatterned shade mask. Both formed under the conditions of a HF concentration of 1.0 wt % and a current density of 2.4 mA/cm^2.

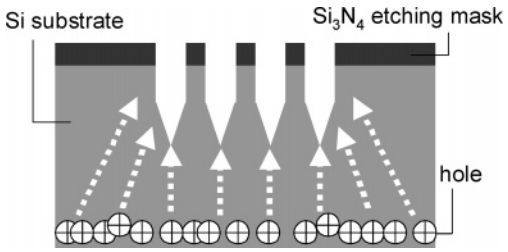

Figure 4. Diffusion model of holes generated in the entire backside of the Si substrate by illumination.

using a halogen lamp (15 V, 150 W) to generate holes. A scanning electron microscope (SEM, Keyence, Real Surface View VE-7800) was used to observe the microstructures formed in the processes.

3. Results and Discussion

First, we attempted to form a macropore array area selectively using the substrate shown in Figure 2a and 2b; in this case, a rim-type Au/Cr pattern was formed on its back surface for only electric contact so that the entire back surface was illuminated.

Figure 3a shows a representative cross-sectional SEM image of the edge part of the area-selectively formed array of the pores. It is apparently seen in Figure 3a that growth rate of the macropores is not uniform; pores located at the edge parts seem to grow faster than those at the inner parts. It is considered that, if the excess amount of holes which were generated at the back surface area, diffused nonlinearly toward the etching area, pores located near the edge parts will receive a larger amount of holes compared with the inner parts, resulting in uneven growth of the macropores, as is schematically shown in Figure 4. To avoid the supply of the excess amount of holes to form a uniform and straight macropore array, a micropatterned Au/Cr shade

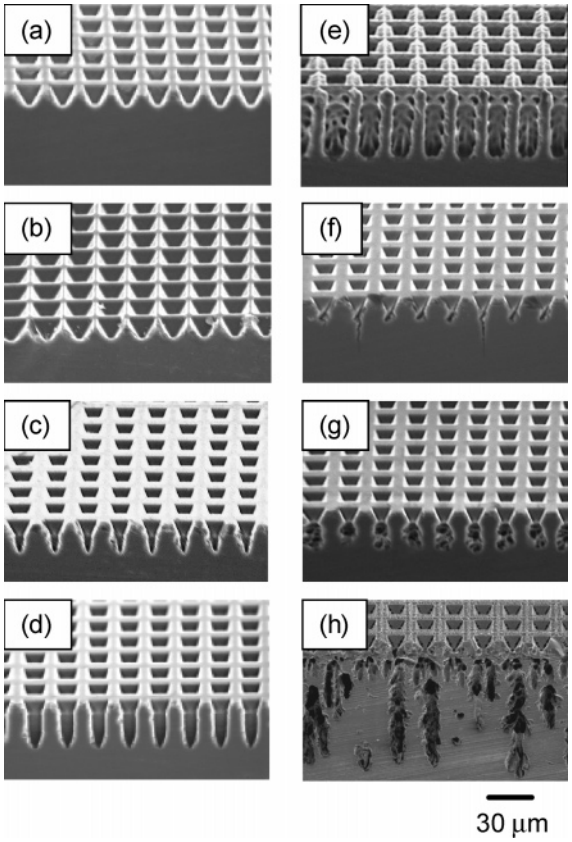

Figure 5. Cross-sectional SEM images showing the effects of HF concentration, current density, and reaction duration; (a) 0.1 wt %, 0.24 mA/cm^2, 480 min; (b) 0.1 wt %, 2.4 mA/cm^2, 120 min; (c) 1.0 wt %, 0.24 mA/cm^2, 480 min; (d) 1.0 wt % 2.4 mA/cm^2, 120 min; (e) 1.0 wt %, 24 mA/cm^2, 120 min; (f) 10 wt %, 0.24 mA/cm^2, 480 min; (g) 10 wt %, 2.4 mA/cm^2, 120 min; (h) 10 wt %, 24 mA/cm^2, 120 min.

mask was applied to the back surface of the specimen, as is shown in Figure 2c. By applying this process, it was confirmed that the uniform and straight macropore array was formed, as is typically seen in Figure 3b. These results indicate that the hole-generation region and hole diffusion to the reaction site are important factors for area-selective formation of macropores.

On the basis of these results, the conditions of the anodization in the system using the shade mask, such as the HF concentration and current density, were optimized.

Figure 5 shows representative cross-sectional SEM images of the specimens prepared under the various conditions. As is seen from Figure 5a and 5b, lower HF concentration such as 0.1 wt % is insufficient for the etching toward the horizontal direction. It is clear that the pitch of the macropore becomes narrower after the anodization under the 0.1 wt % condition, due to a side-etching effect. It is expected that the pores grow toward a vertical direction under the hole transport-limited condition, as is schematically shown in Figure 6a. On the other hand, in the case of F^- transport-limited condition, side-etching like electropolishing proceeds,[21] as is schematically shown in Figure 6b. These conditions can be characterized by critical current density J_{ps}, which is observed as the peak in the anodic polarization curve of Si in the HF solution. J_{ps} can be estimated from following equation:[14]

$$J_{ps} = Cc^{1.5} \exp(-E_a/kT) \quad (1)$$

where the constant C is 3300 A cm^{-2} (wt % HF)$^{-1.5}$, c is HF concentration, the activation energy E_a is 0.345 eV, k is the Boltzmann constant, and T is the temperature.[14] At room

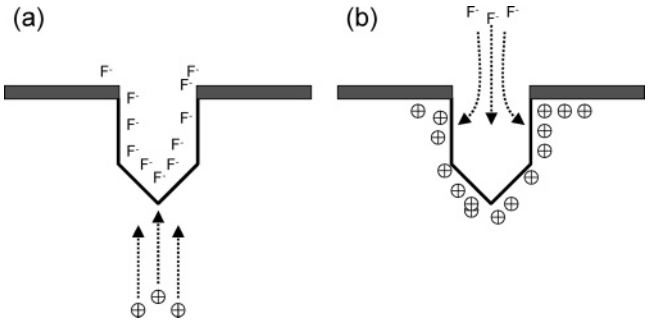

Figure 6. Si dissolution models in aqueous HF solution applying anodic bias; (a) hole transport-limited condition, (b) F^- transport-limited condition.

temperature and a HF concentration of 0.1 wt %, J_{ps} is estimated to be 0.12 mA/cm^2 so that both 0.24 mA/cm^2 and 2.4 mA/cm^2 are larger than the J_{ps}, which indicates that the rate-limiting species in the chemical reaction is F^-, resulting in side-etching like electropolishing. On the other hand, the straight pores were formed in a HF concentration of 1.0 wt %, as is shown in Figure 5c to 5e. Compared with these figures, it is found that the pore diameter formed under low current density is smaller than that under high current density. It is suggested that holes are accumulated at the tip of the micropit at a low current density of 0.24 mA/ cm^2, since the width of the space charge region, which is formed at the surface region of the Si substrate and acts as the Shottky barrier to supply hole, is narrow at the small curvature radius, such as the tip of micropit.[22] On the other hand, at the highest current density of 24 mA/cm^2, the diameter of the macropore is larger than that of the micropit due to the "side-etching" effect, as is shown in Figure 5e, since this current density is larger than J_{ps}, which is calculated at the current density of 4.8 mA/cm^2 and HF concentration of 1.0 wt %. Consequently, the current density around 2.4 mA/cm^2 is expected to be the optimum to form high-aspect-ratio straight pores, since the diameter of the macropore is equal to that of the preformed micropits, indicating that no over-etching to the horizontal direction took place (see Figure 5d). On the other hand, it is confirmed that further increase in the HF concentration resulted in the rough feature of the pore surface, although dissolution of Si seemed to proceed anisotoropically due to lower current density than J_{ps}, which is estimated to be 150 mA/cm^2 at a HF concentration of 10 wt %. In the case of the HF concentration higher than 1.0 wt %, hydrogen-associated Si fluorides, such as $SiH_2(F_2)$ and $SiH_2(SiF)$, are generated and adsorbed on the Si surface,[23] which could inhibit and disorder the hole supply to the reaction site, resulting in a rough feature.

On the basis of the results described above, the HF concentration of 1.0 wt % and current density of 2.4 mA/cm^2 were applied to the following studies to form the array of straight macropores.

To fabricate more than a 100-μm-depth macropore array, we tried the anodization in longer reaction duration, using 625-μm-thick Si wafer.

Figure 7 shows representative cross-sectional SEM images of the specimen with the anodization duration of 1200 min. It is apparent that the depth of the macropores was not uniform. It is suggested that the nonlinear hole diffusion described above resulted in a nonuniform amount of hole supply to each reaction site for the long reaction duration, despite applying the shade mask and the optimum HF concentration and current density. Thus, it is considered that hole diffusion length is also an important factor for formation of a uniform array of macropores in addition to these conditions. To optimize hole diffusion

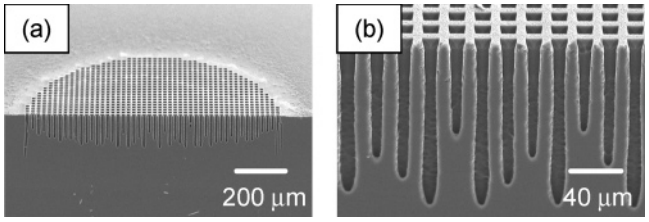

Figure 7. Cross-sectional SEM images of a specimen anodized for 1200 min with 625-μm-thick Si substrate, (a) extensive view of macropore array domain, (b) close-up view of the middle part of the domain.

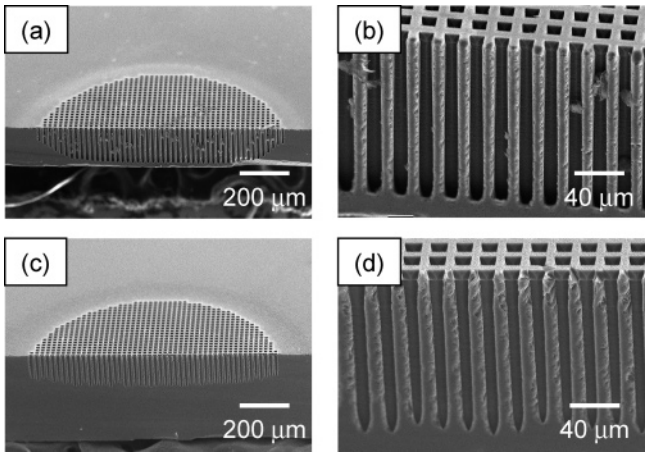

Figure 8. Cross-sectional SEM images of a specimen anodized for 1200 min with different thicknesses of Si substrates, (a) extensive view of the macropore array domain on a 200-μm-thick Si substrate, (b) close-up view of the middle part of the domain on a 200-μm-thick Si substrate, (c) extensive view of the macropore array domain on a 400-μm-thick Si substrate, (d) close-up view of the middle part of the domain on a 400-μm-thick Si substrate.

length, we attempted to adjust the wafer thickness. Figure 8a to 8d shows cross-sectional SEM images of the specimens using 200-μm- and 400-μm-thick Si wafers. From Figure 8a and 8b, it is confirmed that a uniform and straight macropore array was formed in middle part of the domain but that shorter macropores were formed near the edge part. On the other hand, uniform macropores were formed in the entire area with the 400-μm-thick Si wafer, as is shown in Figure 8c and 8d. As a result, it is confirmed that 400-μm-thick Si wafer, the hole diffusion length, is a suitable condition to achieve an even amount of hole supply to every macropore.

From these results, an even-depth and straight macropore array was formed successfully at a selected microarea by controlling the hole generation region, hole supply rate (current density), HF concentration, and hole diffusion length (Si wafer thickness).

4. Conclusion

We have developed the process to form a high-aspect-ratio macropore array at a selected microarea using Si anodization. To avoid the supply of an excess amount of holes to the edge part of the selected area, the shade mask to control the illumination region was applied to the back surface of the Si substrate. As a result, a uniform macropore array was formed. Furthermore, by optimization of the parameters such as HF concentration, current density, and Si wafer thickness, more than a 100-μm-depth macropore array could be formed successfully at the selected area. Since high-aspect-ratio structures are necessary for various nano microsystems, the process developed in this study is expected to be applied to various fabrication processes.

Acknowledgment. This work was financially supported, in part, by the Grant-in-Aid for Scientific Research (C), MEXT, Japan, and performed at the 21st Century Center of Excellence (COE) Program "Practical Nano-Chemistry", MEXT, Japan.

References and Notes

(1) Bustillo, J. M.; Howe, R. T.; Muller, R. S. *Proc. IEEE* **1998**, *86*, 1552.
(2) Spearing, S. M. *Acta Mater*. **2000**, *48*, 179.
(3) Malek, C. K.; Saile, V. *Microelectron. J.* **2004**, *35*, 131.
(4) U.S. Patent 5,501,893.
(5) Yeh, J. L.; Jiang, H.; Tien, N. C. *J. Microelectromech. Syst.* **1999**, *8*, 456.
(6) Chen, K.; Ayón, A. A.; Zhang, X.; Spearing, S. M. *J. Microelectromech. Syst.* **2002**, *11*, 264.
(7) Uhlir, A. *Bell Syst. Technol. J.* **1956**, *35*, 333.
(8) Turner, D. R. *J. Electrochem. Soc.* **1958**, *105*, 402.
(9) Cullis, A. G.; Canham, L. T.; Calcott, P. D. J. *J. Appl. Phys.* **1997**, *82*, 909.
(10) Takai, H.; Ito, T. *J. Appl. Phys.* **1986**, *60*, 222.
(11) Arita, Y.; Kato, K.; Sudo, I. *IEEE Trans. Electron. Devices* **1977**, *ED-24*, 756.
(12) Imai, K. *Solid-State Electron.* **1981**, *24*, 159.
(13) Christophersen, M.; Carstensen, J.; Foll, H. *Phys. Status Solidi A* **2000**, *182*, 103.
(14) Lehmann, V. *J. Electrochem. Soc.* **1993**, *140*, 2836.
(15) Sato, A. *Jpn. J. Appl. Phys.* **2000**, *39*, 378.
(16) Sato, A. *Jpn. J. Appl. Phys.* **2000**, *39*, 1612.
(17) Bertagna, V.; Plougonven, C.; Rouelle, F.; Chemla, M. *J. Electroanal. Chem.* **1997**, *422*, 115.
(18) Smith, R. L.; Chuang, S. F.; Collins, S. D. *J. Electron. Mater*. **1988**, *17*, 533.
(19) Parkhutik, V. P.; Albella, J. M.; Martinez-Duart, J. M.; Gomez-Rodriguez, J. M.; Baro A. M.; Shershulsky, V. I. *Appl. Phys. Lett.* **1993**, *62*, 366.
(20) He, Z. J.; Huang, Y. P.; Kwor, R. *Thin Solid Films* **1995**, *265*, 96.
(21) Foll, H. *Appl. Phys. A* **1991**, *53*, 8.
(22) Beale, M. I. J.; Benjamin, J. D.; Uren, M. J.; Chew, N. G.; Cullis, A. G. *J. Cryst. Growth* **1985**, *73*, 622.
(23) Niwano, M.; Miura, T.; Kimura, Y.; Tajima, R.; Miyamoto, N. *J. Appl. Phys.* **1996**, *79*, 3708.